



## High Q optical resonances of polystyrene microspheres in water controlled by optical tweezers

Julie Lutti, Wolfgang Langbein, and Paola Borri

Citation: [Applied Physics Letters](#) **91**, 141116 (2007); doi: 10.1063/1.2795332

View online: <http://dx.doi.org/10.1063/1.2795332>

View Table of Contents: <http://scitation.aip.org/content/aip/journal/apl/91/14?ver=pdfcov>

Published by the [AIP Publishing](#)

---



## Re-register for Table of Content Alerts

Create a profile.



Sign up today!



# High $Q$ optical resonances of polystyrene microspheres in water controlled by optical tweezers

Julie Lutti, Wolfgang Langbein, and Paola Borri<sup>a)</sup>

*School of Physics and Astronomy, Cardiff University, The Parade, Cardiff CF24 3AA, United Kingdom and School of Biosciences, Cardiff University, Museum Avenue, Cardiff CF10 3US, United Kingdom*

(Received 17 July 2007; accepted 18 September 2007; published online 3 October 2007)

Using evanescent field coupling via frustrated total internal reflection, we measured whispering-gallery optical resonances of polystyrene microspheres held in aqueous buffer by optical tweezers, as a function of the distance from the planar coupling substrate. An intrinsic  $Q$  factor of  $4 \times 10^6$  was found for a microsphere of  $30 \mu\text{m}$  diameter, indicating the potential of such microresonators for highly sensitive biomolecular detection. These measurements provide an upper limit of  $2 \times 10^{-7}$  for the imaginary part of the complex refractive index of polystyrene at  $770 \text{ nm}$  wavelength. © 2007 American Institute of Physics. [DOI: 10.1063/1.2795332]

During the last decade, label-free optical biosensors have become valuable tools for clinical and military use as well as drug discovery. They are important devices for a range of applications going from detection of infectious agents, toxins, proteins, and DNA to investigation of whole cell behavior. Modern label-free optical biosensors, such as the widely utilized surface plasmon resonance (SPR) method,<sup>1</sup> are based on an evanescent light field traveling along a planar surface, probing the target material deposited on the surface. Recently, a novel type of biosensor based on evanescent field coupling has been proposed.<sup>2</sup> This sensor exploits narrow-linewidth photonic resonances of dielectric microspheres (e.g., silica spheres of  $300 \mu\text{m}$  diameter, as in Ref. 2), the so-called whispering-gallery modes (WGMs). These light modes are confined inside the sphere close to its surface by repeated total internal reflection. Molecular binding to the sphere outer surface creates a change of the optical polarizability in the evanescent field of the WGMs, which is detected as a change in the resonance wavelength. Since the light in WGMs can orbit many thousand times before escaping the resonator, the detection sensitivity of this method as compared to planar surface-based methods is expected to be greatly enhanced.<sup>3,4</sup>

We have developed an experimental setup to measure WGM resonances of polystyrene microspheres (PMs) held in aqueous buffer by optical tweezers, at a controlled distance from a glass substrate. With this setup, we detected sharp WGM resonances limited only by the intrinsic linewidth broadening, rather than by coupling to the substrate,<sup>5</sup> with  $Q$  factors as high as  $4 \times 10^6$  for a microsphere of  $30 \mu\text{m}$  diameter at  $770 \text{ nm}$  wavelength, promising for biosensing applications.

In our experiment, microspheres are injected into a homebuilt flow chamber with controlled fluidic delivery and two-side optical access (see Fig. 1). The optical tweezers are created by a hollow cone of light at large angle obtained by focusing an annular beam with a high numerical aperture ( $\text{NA}=1.3$ ) microscope objective. The annular beam profile is shaped from a  $\text{TEM}_{00}$  mode of a Nd:YAG (yttrium aluminum garnet) continuous wave laser at  $1064 \text{ nm}$  wavelength by a pair of axicons. A geometrical optics calculation<sup>6</sup> shows

that the axial trapping force is doubled compared to a full cone illumination of equal aperture and power.<sup>7</sup> Additionally, the annular illumination facilitates the use of a standard oil immersion objective for trapping in water by reducing the impact of spherical aberrations created by the refractive index mismatch. Using a cone angle of  $64^\circ$  and a power of  $250 \text{ mW}$ , PMs of  $15\text{--}40 \mu\text{m}$  diameter were trapped through  $\sim 80 \mu\text{m}$  of water from the chamber side near the objective. The gravitational force acts along the  $y$  axis which is transverse to the axial trapping direction ( $z$  axis). In those conditions, thermal position fluctuations of the PMs along the axial trapping direction were calculated to be  $\approx 25 \text{ nm rms}$ , which is smaller than the WGM evanescent field decay length and thus sufficient to control the coupling to the substrate. The position of the objective was controlled by a mechanical stage of  $20 \text{ nm}$  resolution, allowing calibrated axial movement of the trap, and thus of the distance  $z$  between the PM and the substrate.

WGMs were optically excited using a tunable distributed feedback (DFB) laser emitting at a wavelength  $\lambda$  around

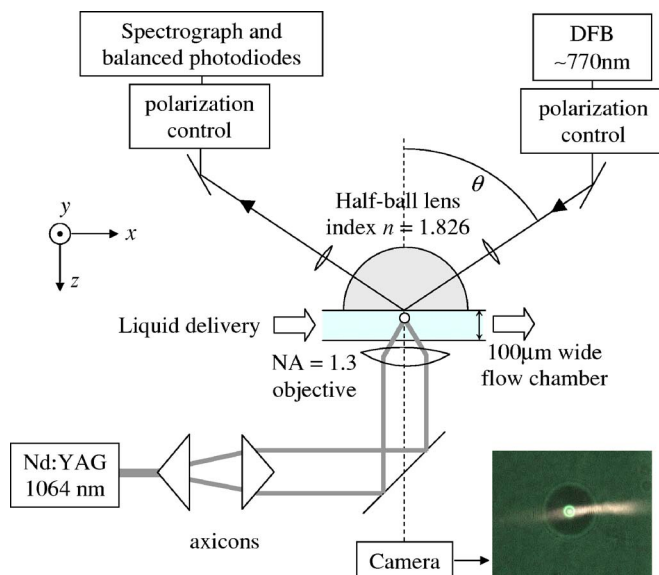


FIG. 1. (Color online) Sketch of the experimental setup. The  $y$  direction indicates the vertical direction in the laboratory system. The image shows a trapped PM coupled to the excitation beam.

<sup>a)</sup>Electronic mail: borri@cardiff.ac.uk

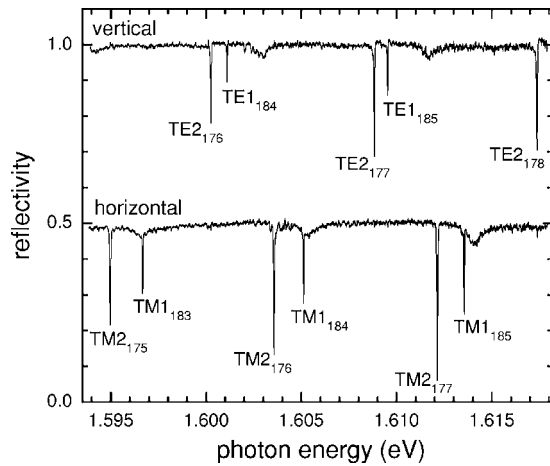


FIG. 2. TE and TM polarized reflectivity spectra of a  $30\ \mu\text{m}$  PM at a distance to the substrate of about  $400\ \text{nm}$ . The TM spectrum is displaced vertically by 0.5 for clarity. The resonances are labeled by the WGM order  $n$  and number  $\ell$  in the subscript.

$770\ \text{nm}$ , corresponding to a photon energy of  $\hbar\omega \sim 1.60\ \text{eV}$ . The beam is focused onto the planar interface between a high index half ball lens (the substrate) and water, where it is totally internally reflected. When a PM is positioned in the evanescent field of the reflection spot, the exciting beam couples to the WGMs. The spot diameter of  $\sim 5\ \mu\text{m}$  and the excitation angle  $\theta \sim 55^\circ$  were adjusted to optimize the coupling to the WGMs, which are detected as dips in the measured reflectivity spectrum. Both horizontal ( $x$ ) and vertical ( $y$ ) polarizations, which couple respectively to the transverse magnetic (TM) and transverse electric (TE) WGMs, are detected. A DFB laser operating below threshold provides a spectrally broad emission which is used for excitation of WGMs over a spectral range of several tens of meV. The reflection is dispersed by a high-resolution ( $\sim 6\ \mu\text{eV}$ ) grating spectrometer and detected by a cooled charge coupled device (CCD) camera. Above threshold, the DFB laser emission is ultranarrow ( $16\ \text{neV}$ ) and can be temperature tuned over a range of  $5\ \text{meV}$  as well as rapidly scanned over  $100\ \mu\text{eV}$  using a triangular current modulation at about  $50\ \text{Hz}$ . In this case, the detection uses two photodiodes and an oscilloscope to measure the difference between the vertically and horizontally polarized reflected intensities.

Reflectivity spectra measured with the CCD camera on a PM held in aqueous buffer are shown in Fig. 2. We used a batch of PMs of  $24$  to  $31\ \mu\text{m}$  diameter (Polysciences, Inc.) in purified water with surfactant (Triton X-100) at a volume concentration of  $10^{-4}$ , added to avoid sphere aggregation and attachment to the glass substrate. The sharpest resonances are attributed to  $n=1$  WGMs, where  $n$  is the mode order. Accurate determination of the sphere diameter and identification of mode numbers  $\ell$  of the WGMs were made by comparison of the resonance energies with calculated WGM energies using explicit asymptotic formulas.<sup>8</sup> For the PM in Fig. 2, the diameter is determined to be  $30.1 \pm 0.2\ \mu\text{m}$ , using a refractive index<sup>9</sup>  $n_p = 1.58 \pm 0.005$  at  $\lambda = 770\ \text{nm}$ .

By varying the excitation angle  $\theta$  (see Fig. 1) in order to maximize the TE1 resonance amplitude at a fixed distance between PM and substrate, we determined an optimum excitation angle of  $\theta = 55 \pm 3^\circ$  for PMs of  $\sim 30\ \mu\text{m}$  diameter. At this angle, the effective in-plane refractive index of the excitation is  $n_x = n_b \sin \theta = 1.50 \pm 0.05$  with the substrate refractive

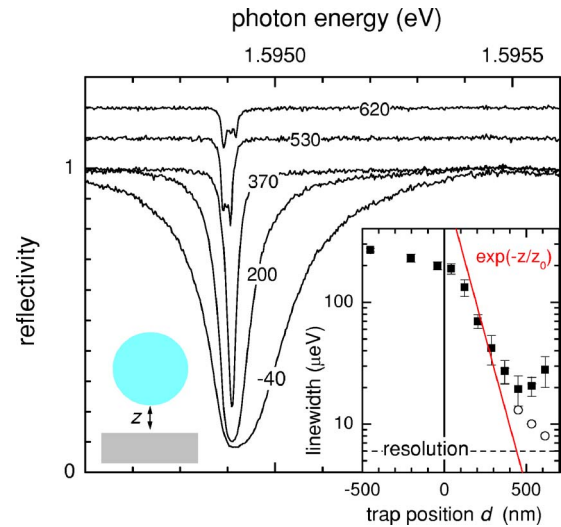


FIG. 3. (Color online) Reflectivity spectra around the TE1<sub>172</sub> mode for a PM of  $28.4\ \mu\text{m}$  diameter at varying distances to the substrate. Curves are labeled with the corresponding trap position  $d$  in nanometers. Inset: measured linewidth vs.  $d$ . Solid squares are FWHM with error bars being the standard deviation from a Lorentzian fit over a time series. Circles are widths of the sharpest subresonances. The solid line indicates the expected dependence (see text), and the dashed line the spectrometer resolution.

index  $n_b = 1.826$ . This matches the effective index of the WGM given by  $n_{\text{eff}} = \ell / (Rk_0) = 1.50 \pm 0.01$  for PM diameters  $2R$  of  $24$  to  $31\ \mu\text{m}$ , where  $k_0 = 2\pi/\lambda$  is the wave vector in vacuum. All data shown in this letter have been measured with  $\theta$  in this range.

Figure 3 shows the reflectivity, measured with the CCD camera, for a TE1 resonance when varying the position of the trap  $d$  over a range from physical contact between PM and substrate ( $d \leq 0$ ) to negligible coupling with the evanescent field. At large  $d$ , the measured resonance consists of several narrow lines. These multiple lines arise from the lifting of the degeneracy of the  $2\ell + 1$  azimuthal modes for PMs deviating from perfect sphericity, as previously observed for smaller polystyrene beads.<sup>10</sup> By approaching the substrate, the resonance becomes deeper and broader and the lifting of the degeneracy becomes indiscernible. The depth increases all the way to contact with the substrate, different from other reports of depth reduction, once the optimum coupling condition is surpassed, i.e., when the linewidth due to the coupling is larger than the intrinsic linewidth.<sup>5,11</sup> This difference is due to our detection being sensitive only to the intensity within the spatial mode of the reflected excitation without PM, and not to the intensity in other substrate modes into which the WGM couples. Note that the distance  $z$  follows the trap position only for large distances. When the PM touches the substrate, its position is affected by interactions between its surface and the substrate. This interaction depends on the specific surface shape and is sensitive to the surfactant and contaminations. In the inset of Fig. 3, the WGM linewidth is given as a function of the trap position  $d$ , where the zero is taken at the onset of linewidth saturation, with an estimated error of  $\pm 50\ \text{nm}$ . The linewidth saturates for  $d < 0$  as  $z$  approaches zero. From the saturation behavior, we estimate that  $z = d$  holds for  $d > 100\ \text{nm}$ .

The WGM linewidth  $\gamma_c$  due to the photon escape into the bulk modes of the substrate is expected to be exponentially dependent on  $z$ ,  $\gamma_c \propto \exp(-z/z_0)$ , with a decay length  $z_0$  given by the evanescent field intensity decay of the excited

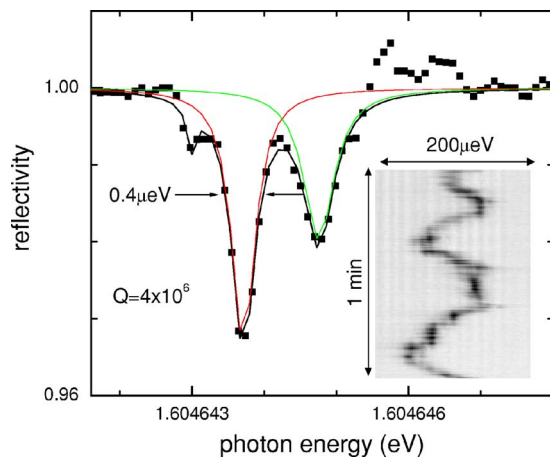


FIG. 4. (Color online) Reflectivity spectrum of a  $TM_{1184}$  resonance of a PM of  $30.1 \mu\text{m}$  diameter, measured by scanning the DFB. The spectrum is fitted by a sum of three Lorentzian curves (lines). Inset: reflectivity of the same microsphere as a function of time on a gray scale from 0.2 (black) to 1 (white).

WGM.<sup>5</sup> From the effective index  $n_{\text{eff}}$  we can calculate  $z_0 \approx 88 \text{ nm}$  using  $(2z_0)^{-2} = (n_{\text{eff}}^2 - n_w^2)k_0^2$ , with the refractive index of water  $n_w = 1.33$ . The resulting  $\gamma_c$  versus  $z$  is given in the inset of Fig. 3, showing a significantly stronger dependence on  $z$  than the measured linewidths. We attribute this finding to the lifting of the mode degeneracy in the experiment, introducing an additional broadening. By analyzing the linewidth of individual nondegenerate modes possible for distances above  $500 \text{ nm}$ , we find widths eventually limited by the spectrometer resolution (open circles in the inset).

We have used the scanning DFB detection to resolve the spectrum at a large distance  $z \approx 700 \text{ nm}$ , in a regime where the WGM linewidth was observed not to be significantly influenced by the coupling to the substrate, i.e., in its intrinsic limit. A resulting high-resolution spectrum for a  $TM_{1184}$  mode in a PM of  $30.1 \mu\text{m}$  diameter is given in Fig. 4. The strongest observed peak has a linewidth [full width at half maximum (FWHM)] of  $\gamma = 0.4 \mu\text{eV}$  ( $0.2 \text{ pm}$ ), and thus a  $Q$  factor  $\hbar\omega/\gamma = 4 \times 10^6$ , the highest measure for a polystyrene microsphere. From this value we can calculate the photon storage time in the mode  $\tau = Q/(k_0c)$ , with the speed of light  $c$ , yielding  $\tau = 1.6 \text{ ns}$ . Neglecting absorption and scattering losses, the  $Q$  factor of a  $30 \mu\text{m}$  diameter PM in water is calculated using Mie theory to be  $Q = 1.5 \times 10^8$ , much larger than the measured one. The absorption by water<sup>12</sup> at  $770 \text{ nm}$  is about  $2.5 \text{ m}^{-1}$ , only reducing the  $Q$  factor to  $1.3 \times 10^8$  considering the small mode fraction of 4% in water. The intrinsic absorption in polystyrene at  $770 \text{ nm}$  is dominated by C–H overtone absorption, and can be estimated by the typical losses of polymer fibers<sup>13</sup> of less than  $1000 \text{ dB/km}$ , corresponding to an absorption coefficient of  $0.23 \text{ m}^{-1}$ . This absorption would reduce the  $Q$  factor to about  $5 \times 10^7$ . We therefore believe that Rayleigh scattering (e.g., by surface roughness) still dominates the observed  $Q$  factor. Independent of this interpretation, the measured  $Q$  factor gives an upper limit for the absorption coefficient of polystyrene of  $\alpha = n_p/c\tau = 3.2 \text{ m}^{-1}$  at  $770 \text{ nm}$ , corresponding to an imagi-

nary part of the complex refractive index of  $\kappa = \lambda\alpha/4\pi = 2 \times 10^{-7}$ .

We should comment that while the microsphere rotates freely inside the optical trap, the spatially localized excitation couples for different rotation angles to different subensembles of nondegenerate azimuthal modes which are solidal to the PM, so that the weight of different modes in the reflection spectrum changes with time. This is illustrated in the inset of Fig. 4, where the reflectivity measured over a longer time period is shown. The observed oscillatory structure is attributed to a cyclic rotation dynamics of the sphere induced by a residual flow of the surrounding liquid. We found that the spectral position of individually resolved resonances is unchanged with time, while their amplitude varies. This confirms that the measured dynamics in the reflection spectrum is due to a changing coupling strength to individual modes as opposed to a change of the dielectric properties of the surrounding medium. The total spectral range of the measured ensemble of resonances was typically less than  $200 \mu\text{eV}$ , which corresponds to a PM asphericity in the  $10^{-4}$  range.

In conclusion, we have measured WGM resonances with a  $Q$  factor as high as  $4 \times 10^6$  on a  $30 \mu\text{m}$  diameter polystyrene microsphere held in aqueous buffer by optical tweezers. Such sharp resonances could be used for sensitive detection of refractive index changes or biomolecule attachment.<sup>2–4</sup> For practical applications the microsphere should be fixed instead of being free to rotate to avoid mode jumping. Work is in progress to develop a planar separation layer from the substrate onto which the PM will be glued. Assuming that the minimum detectable wavelength shift is  $1/25$  of the WGM linewidth, we estimate a sensitivity to a refractive index change in the surrounding medium of  $4 \times 10^{-7}$ . Finally, for biosensing applications using the expression developed in Ref. 3, we infer a protein detection sensitivity of  $0.25 \text{ pg/mm}^2$  in terms of surface mass loading and  $0.7 \text{ fg}$  in terms of minimum detectable total mass loading, significantly better than those in conventional SPR methods.<sup>1</sup>

This work is funded by the UK Ministry of Defence (Dstl) under Contract No. RD031-011961. The authors acknowledge discussions with Martin McDonnell.

<sup>1</sup>B. Liedberg, I. Lundström, and E. Stenberg, *Sens. Actuators B* **11**, 63 (1993).

<sup>2</sup>F. Vollmer, D. Braun, A. Libchaber, M. Khoshshima, I. Teraoka, and S. Arnold, *Appl. Phys. Lett.* **80**, 4057 (2002).

<sup>3</sup>S. Arnold, M. Khoshshima, I. Teraoka, S. Holler, and F. Vollmer, *Opt. Lett.* **28**, 272 (2003).

<sup>4</sup>I. Teraoka, S. Arnold, and F. Vollmer, *J. Opt. Soc. Am. B* **20**, 1937 (2003).

<sup>5</sup>M. L. Gorodetsky and V. S. Ilchenko, *J. Opt. Soc. Am. B* **16**, 147 (1999).

<sup>6</sup>A. Ashkin, *Biophys. J.* **61**, 569 (1992).

<sup>7</sup>Assuming the dielectric spheres having a diameter much larger than the diffraction limited trap focus size and a small difference of refractive index relative to the surrounding medium [J. Lutti, W. Langbein, and P. Borri (unpublished)].

<sup>8</sup>C. C. Lam, P. T. Leung, and K. Young, *J. Opt. Soc. Am. B* **9**, 1585 (1992).

<sup>9</sup>I. D. Nikolov and C. D. Ivanov, *Appl. Opt.* **39**, 2067 (2000).

<sup>10</sup>N. Le Thomas, U. Woggon, W. Langbein, and M. V. Artemyev, *J. Opt. Soc. Am. B* **23**, 2361 (2006).

<sup>11</sup>M. Cai, O. Painter, and K. J. Vahala, *Phys. Rev. Lett.* **85**, 74 (2000).

<sup>12</sup>G. M. Hale and M. R. Querry, *Appl. Opt.* **12**, 555 (1973).

<sup>13</sup>E. Nihei, T. Ishigure, and Y. Koike, *Appl. Opt.* **35**, 7085 (1996).